

# TASM: A Tile-Based Storage Manager for Video Analytics

Maureen Daum

Paul G. Allen School of Computer  
Science & Engineering  
University of Washington  
mdaum@cs.washington.edu

Brandon Haynes

Paul G. Allen School of Computer  
Science & Engineering  
University of Washington  
bhaynes@cs.washington.edu

Dong He

Paul G. Allen School of Computer  
Science & Engineering  
University of Washington  
donghe@cs.washington.edu

Amrita Mazumdar

Paul G. Allen School of Computer  
Science & Engineering  
University of Washington  
amrita@cs.washington.edu

Magdalena Balazinska

Paul G. Allen School of Computer  
Science & Engineering  
University of Washington  
magda@cs.washington.edu

Alvin Cheung

Department of Electrical Engineering  
and Computer Sciences  
University of California, Berkeley  
akcheung@cs.berkeley.edu

## ABSTRACT

The amount of video data being produced is rapidly growing. At the same time, advances in machine learning and computer vision have enabled applications to query over the contents of videos. For example, an ornithology application may retrieve birds of various species from a nature video. However, modern video data management systems store videos as a single encoded file, which does not provide opportunities to optimize queries for spatial subsets of videos. We propose utilizing a feature in modern video codecs called “tiles” to enable spatial random access into encoded videos. We present the design of TASM, a tile-based storage manager, and describe techniques it uses to optimize the physical layout of videos for various query workloads. We demonstrate how TASM can significantly improve the performance of queries over videos when the workload is known, as well as how it can incrementally adapt the physical layout of videos to improve performance even when the workload is not known. Layouts picked by TASM speed up individual queries by an average of 51% and up to 94% while maintaining good quality.

## 1 INTRODUCTION

The amount of video data being created is rapidly growing. YouTube alone has more than 400 hours of video uploaded every minute [49]. At the same time, advances in machine learning and computer vision have enabled new applications on video data such as automatic traffic analysis [32, 53], retail store planning [26], and drone analytics [47, 48]. This has led to a class of database systems specializing in video data management that facilitate query processing over videos [22, 27, 28, 40, 52, 54].

Thanks to the advent of deep learning, these new video database management systems (VDBMSs) enable applications to ask questions about the contents of a video. While some applications may ask statistical questions (e.g., “How many cars passed through this intersection yesterday?”), many issue queries to retrieve relevant video fragments. For example, an amber alert application may need to retrieve all sequences showing a vehicle that matches a given description and has a specific license plate. An ornithology application may search for birds of a given species in a nature video. These queries require a system to return not only a desired subset of frames but only specific pixels within those frames. When applications retrieve video fragments, users may issue many queries

before finding the desired content. For example, an ornithologist may be looking for a sequence of hummingbirds feeding on specific flowers, issuing a variety of queries for hummingbirds and flowers.

These types of queries are expensive to execute, and modern VDBMSs optimize them in a variety of ways. Consider a specific query issued by an amber alert application to find blue vans. A VDBMS could optimize this query by reducing the number of expensive operations it performs. For example, color detection is cheaper than object detection, so it could only run object detection on regions with a lot of blue pixels. It could use techniques from NoScope [28] to swap out the expensive general-purpose object detector for a cheaper model that is specialized to recognize vans. It could also reduce video quality (e.g., by using VStore [52]) so that it is less expensive to apply object recognition or license plate detection.

In all these cases, however, before a VDBMS can run operations over the contents of a video file, it must first decode and decompress the video to recover the raw frame data from the compressed representation. This process is expensive—especially for high-resolution videos—but cannot be avoided because uncompressed video is usually orders of magnitude larger than its compressed counterpart [50]. Additionally, current video storage methods require decompressing complete video frames and do not enable efficient retrieval of relevant spatial subsets of those frames. This lack of spatial random-access points ultimately hurts the performance of queries that do not require the contents of entire frames.

In this paper, we develop a new storage manager for video data that accelerates content-based retrieval operations on video files. The goal of our storage manager, called TASM, is to be the bottom layer of a VDBMS and to rapidly return video fragments containing objects of interest. The key idea behind our approach is to optimize how a video is stored on disk to reduce the amount of work spent decoding parts of the video not involved in a query. For example, the amber alert application targets just the blue vans in a video, so the time spent by a VDBMS decoding or otherwise processing other pixels should be minimized. To optimize the video layout on disk, TASM needs to know the location of objects of interest in the video. To avoid unnecessary overheads, TASM learns that information incrementally as applications execute queries over the video.

TASM uses a new feature of modern video codecs, called *tiling*. TASM’s first contribution is to leverage this feature when storing video data and to optimize how a video is tiled based on its

content and query workload. Tiling enables the partitioning of each video frame following a configurable grid, such that each grid cell becomes an independently encoded (and decodable) tile. The key technical challenge is to develop an approach that (1) automatically determines if tiling will be beneficial to query execution, (2) optimizes the choice of tiling for a video fragment based on a given query workload, and (3) incrementally tiles a video as information about the content of the video and the target of queries over the video becomes known. TASM addresses these challenges. It introduces a cost function to determine the cost-effectiveness of tiling a video fragment. It estimates the retiling cost and the benefit of different tile layouts for a given query and uses these cost estimates to select the optimal tiling for a given query workload.

To support its tiling decisions, TASM uses a semantic index to store information about a video’s content. By contrast, VDBMSs typically fail to take advantage of useful information about the video generated while analyzing it. Large intermediate results created by the analysis algorithms while executing a query are often discarded. For example, if an application submits a query to detect license plates, a VDBMS will learn something about the locations of cars in the video as it processes the query. This information about the contents of the video can not only be used in future queries to avoid re-running expensive models, but it can also be used by the system to decide which parts of the video should be optimized for fast access. To make use of this information, we propose building a *semantic index* over videos using metadata (e.g., object bounding boxes, color, locations). The semantic index incorporates information generated about the video during preprocessing steps via computational or human-driven analysis techniques, as well as information generated during query processing. TASM uses the semantic index in its video layout optimization process.

For most videos, neither the queries nor the objects in the video are known ahead of time. The second contribution of TASM is to introduce algorithms to address this challenge. TASM tiles videos incrementally, not only by using different tile layouts in different parts of the video, but also by evolving the tile layout in individual sections of the video over time. Incremental tiling, however, can be expensive and can slow down query execution. For example, if TASM tiles part of a video around cars but the next query retrieves pedestrians, the tile layout designed around cars could cause the query for pedestrians to execute more slowly than if the video were not tiled at all. Encoding a video with tiles is expensive, so picking a bad layout can not only slow down future queries, but also waste time spent on encoding. To address this uncertainty, TASM uses techniques inspired by database cracking [15, 24] and online indexing [11] to decide when to re-tile portions of the video and with which layouts. TASM accumulates estimated performance improvements offered by various tile layouts as it observes queries. Once the estimated improvements of a new layout offset the cost of re-encoding, TASM re-tiles that portion of the video. By observing multiple queries before making tiling decisions, TASM can design layouts optimized for multiple query types. For example, TASM could tile around cars *and* pedestrians to speed up queries for both objects.

The third contribution of TASM is its judicious use of edge computing. Edge cameras generate video for VDBMSs, but also have the computational power to run object detection on-device [3]. For some applications, a VDBMS will know which objects will be

targeted by queries in advance (e.g., an amber alert application will primarily target cars), but not where these objects are in the video. To leverage this partial knowledge, we augment TASM by utilizing the computational power of edge cameras to detect objects as the video is captured. The camera initially encodes the video with tiles to reduce the encoding work required when the video is later loaded into a VDBMS, as the system will not have to re-encode the video with tiles. Initially encoding the video with tiles can also reduce the amount of data the edge device sends to the cloud for processing because it can choose to stream only the tiles that contain objects.

In summary, the contributions of this paper are:

- Developing TASM, a new type of storage manager for video data that has two components: a semantic index and a tile layout generator. TASM splits video frames into independently queryable tiles, and it optimizes the layout of a video file based on its content and the query workload. By doing so, TASM accelerates queries that retrieve objects in videos while keeping storage overheads low and maintaining good video quality.
- Developing new algorithms for TASM to dynamically evolve the video layout as information about the video content and query workload becomes available over time.
- Extending TASM with edge computing capabilities to accelerate query processing for the case where objects that are targeted by queries are known ahead of time.
- Evaluating TASM on a variety of videos and workloads and demonstrating that the layouts picked by TASM speed up individual queries by an average of 51% and up to 94% while maintaining good quality, and that TASM can automatically tune layouts over a small number of queries to improve performance even when the workload is unknown.

## 2 BACKGROUND

Videos are stored as encoded files due to their large size. Video codecs such as H264 [1], HEVC [4], and AV1 [2] specify encoding and decoding algorithms used to (de)compress videos. While the specific algorithms used by various codecs differ, the high-level approach is the same as we describe in this section.

**Groups of pictures:** A video consists of a sequence of frames, where each frame is a 2D array of pixels. Frames in the sequence are partitioned into *groups of pictures* (GOPs). Each GOP is encoded independently from the other GOPs and is typically one second in duration. The first frame in a GOP is called a *keyframe*. Keyframes allow GOPs to act as temporal random access points into the video because it is possible to start decoding a video at this initial keyframe. To retrieve a specific frame, the decoder can start decoding at the closest keyframe preceding the frame being retrieved. Keyframes have large storage sizes because they use a less efficient form of compression than other types of frames, so the number of keyframes impacts a video’s overall storage size. Videos stored with long GOPs are smaller in size than videos stored with short GOPs, but they also have fewer random access opportunities.

**Tiles:** Compressed videos do not generally support decoding spatial regions of a frame. The encoding process creates dependencies between different regions of a frame, and decoders must resolve these dependencies by decoding the entire frame,

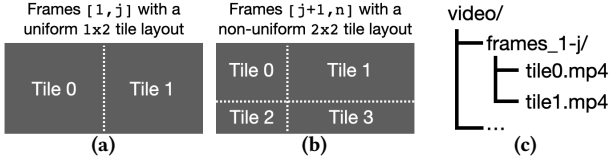


**Figure 1: Video partitioned into tiles.** (a) shows the first  $j$  frames partitioned with a uniform  $1 \times 2$  layout. (b) shows frames partitioned using a non-uniform  $2 \times 2$  layout. (c) shows a directory hierarchy. Video stored at `video/frames_1-j/tile0.mp4` contains the left half of frames  $[1, j]$ .

even if just a small region is requested. Modern codecs, however, provide a feature called *tiles* that enables splitting frames into independently-decodable regions. Figure 1 illustrates this concept. Tiles introduce spatial random access points for decoding. To decode a region within a frame, the decoder can process only the tiles that contain the requested region. This flexibility to decode spatial subsets of frames comes with tradeoffs in quality; tiling can lead to artifacts appearing at the tile boundaries [44], which can reduce the visual quality of videos. As such, carefully selecting tile layouts is important for high quality query results. While tiles act as spatial random access points, temporal random access is still provided by keyframes. Tiles are applied to all frames within a GOP, so decoding a tile in a non-keyframe requires decoding that tile in all frames starting from the preceding keyframe.

A *tile layout* defines how a sequence of frames is divided into tiles. A layout  $L = (n_r, n_c, \{h_1, \dots, h_{n_r}\}, \{c_1, \dots, c_{n_c}\})$  is defined by the number of rows and columns,  $n_r$  and  $n_c$ , the height of each row, and the width of each column. These parameters define the  $(x, y)$  offset, width, and height of the  $n_r \cdot n_c$  tiles. An untiled video is a special case of a tile layout consisting of a single tile that encompasses the entire frame:  $\omega = (1, 1, \{frame\_width\}, \{frame\_height\})$ . Valid layouts require tiles to be partitioned along a regular grid, meaning rows and columns extend through the entire frame. We do not consider irregular layouts, which are not supported by the HEVC specification [4]. Different tile layouts can be used throughout the video; a *sequence of tiles* (SOT) refers to a sequence of frames with the same layout. Changes in the layout must happen at GOP boundaries, so every new layout must start at a keyframe, which have poor compression performance. This leads to a high storage overhead of changing the tile layout. The cost of executing a query over a video encoded with tiles is proportional to the number of pixels and tiles that are decoded.

**Stitching:** Tiles can be stored separately, but they must be combined to recover the original video. Tiles can be combined without an intermediate decode step using a process called *homomorphic stitching* [17]. Homomorphic stitching interleaves the encoded data from each tile and adds header information so the decoder knows how the tiles are arranged.

### 3 TILE-BASED STORAGE MANAGER DESIGN

In this section, we present the design of TASM, our tile-based storage manager. TASM is designed to be the lowest layer in a modern VDBMS. Unlike existing storage managers that serve requests for sequences of frames, TASM can efficiently retrieve regions *within* frames to answer queries for specific objects. By doing so, TASM accelerates these types of queries.

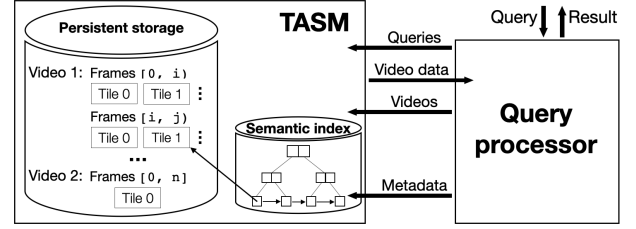


**Figure 2: Overview of how TASM integrates with a VDBMS.**

Figure 2 shows an overview of how TASM integrates with the rest of a VDBMS. TASM utilizes a *semantic index* to store the bounding boxes associated with object detections and map each bounding box to the tiles that contain it. TASM performs two main tasks to accelerate queries for specific objects. First, it incrementally populates the semantic index using object detections that are produced as a byproduct of query execution. Each detection is a bounding box and one or more labels provided by the query processor as metadata. Second, it uses this index to generate tile layouts, split videos into tiles, store such physically tuned videos as files on disk, and answer queries more efficiently by retrieving only relevant subsets of data from disk.

#### 3.1 TASM API

TASM exposes an access method API. The core method `SCAN(video, L, T)` retrieves the pixels that satisfy a predicate on the labels,  $L$ , and an optional predicate on the time dimension,  $T$ . As an example,  $L = (label = 'car') \vee (label = 'bicycle')$  retrieves pixels for both cars and bicycles, while  $L = (label = 'car') \wedge (label = 'red')$  retrieves pixels belonging to red cars.  $L$  can be any CNF predicate. For each disjunctive clause  $c = l_0 \vee \dots \vee l_n$ , TASM retrieves pixels that lie in the bounding boxes associated with any  $l_i$ . For each conjunction,  $L = c_0 \wedge \dots \wedge c_n$ , TASM retrieves pixels that lie in the intersection of bounding boxes associated with all  $c_i$ . If the predicate  $T = t_{start} \leq t < t_{end}$  or  $T = t$  is specified, TASM only considers frames that lie in the specified temporal range.

TASM also exposes an API to incorporate metadata generated during query processing into the semantic index (discussed in the following section). The method `ADDMETADATA(video_id, frame, label, x1, y1, x2, y2)` adds the bounding box  $(x_1, y_1, x_2, y_2)$  on *frame* to the semantic index and associates it with the specified label.

#### 3.2 Semantic index

TASM maintains metadata about the contents of videos in a *semantic index*. The semantic information takes the form of labels associated with bounding boxes. Labels denote object types and properties such as color. Bounding boxes locate an object within a frame. The search key of the index is a video identifier, a time within the video, a label of interest, and an associated bounding box. The value in the index is a pointer to the underlying tile on disk. When the query processor invokes TASM's `SCAN(v, L, T)` method, TASM must be able to efficiently retrieve bounding box information associated with the labels in  $L$  and within the time range specified by  $T$ . The semantic index is therefore implemented as a B-tree clustered on  $(video, label, time)$ . The leaves contain information about the

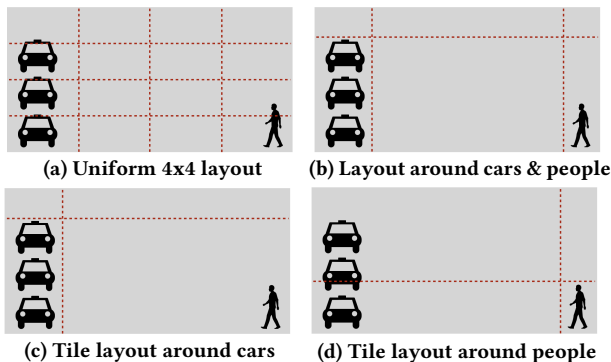


Figure 3: Various ways to tile a frame. (a) is a uniform layout, while (b)-(d) are non-uniform layouts. Depending on which objects are targeted, different layouts will be more efficient.

bounding boxes and pointers to the encoded video tile(s) each box intersects based on the associated tile layout.

To illustrate, consider the amber alert example in Section 1. Imagine TASM tiles the video *traffic* around cars for the time range  $[s, e]$ . When a user queries for suspicious vehicles from  $[s, e]$ , the query processor invokes TASM’s SCAN (*traffic, car, s ≤ time < e*) method. TASM searches the semantic index using the same predicates to find the regions that must be returned to the query processor, and the tiles that contain these regions. It then returns the pixels that match the query predicate. A spatial index could further accelerate queries containing conjunctive predicates by efficiently computing the intersection of bounding boxes before fetching tiles.

### 3.3 Building the semantic index

The semantic index is populated through the ADDMETADATA method as the query processor detects objects in the video. A VDBMS can detect objects in numerous ways. It can run a user- or system-specified general-purpose object detector, such as YOLOv3 [42]. Alternatively, the system could use specialized models for the specific object classes targeted by queries [27, 28] or for specific properties of the videos being queried [25]. These techniques can be used at query time, or the VDBMS can perform some amount of object detection at ingest time to speed up future queries. We explore the tradeoffs between incrementally populating the semantic index at query time and eagerly populating it at ingest time in Section 4.

### 3.4 Tile-based data storage

Having captured the metadata about objects and other interesting areas in a video using the semantic index, the next step is to leverage it to guide how the video data is encoded with tiles. Two approaches are possible for splitting a video into tiles: uniform-sized tiles, or non-uniform tiles whose dimensions are set based on the locations of objects in the video. Both techniques can improve query performance, but tile layouts that are designed around the objects in frames can reduce the number of non-object pixels that have to be decoded. Figure 3 shows these different tiling strategies on an example frame that contains cars and pedestrians.

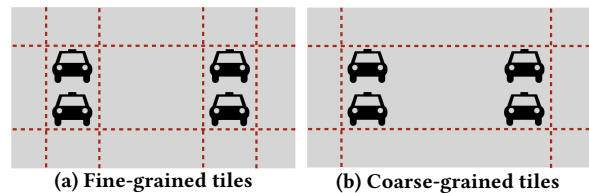


Figure 4: Non-uniform tile layout around cars using (a) fine-grained tiles, or (b) coarse-grained tiles.

**3.4.1 Uniform layouts.** The uniform layout approach divides frames into tiles with equal dimensions. This approach does not leverage the semantic index, so the video can be tiled before any metadata is generated. If objects in the video are small relative to the total frame size, they will likely lie in a subset of the tiles. Therefore, queries to retrieve objects from the video can be executed by decoding just a subset of tiles. However, because the tile layout does not consider the locations of objects in the video, an object can intersect multiple tiles with part of the object in each tile, as shown in Figure 3(a) where a part of the person lies in two tiles. While TASM can decode fewer pixels than the entire frame, it still must decode many pixels that are not requested by the query. Moreover, because the tile layouts do not consider the locations of objects, tile boundaries could intersect objects and degrade their visual quality. Further, the quality of entire frames is reduced because in general, a large number of uniform tiles are required to improve query performance, as shown in Figure 6(b).

**3.4.2 Non-uniform layouts.** TASM creates non-uniform layouts with tile dimensions such that objects targeted by queries lie within a single tile. Figure 4 shows examples of non-uniform tile layouts around cars. For a given video, set of objects  $O$ , a sequence of tiles (SOT; see Section 2) from frames  $[f_a, f_b]$ , and a set of bounding boxes  $B$ , TASM designs tile boundaries around  $B$  guided by a desired tile granularity. For coarse-grained tiles (Figure 4(b)), it places all  $B$  within a single, large tile. For fine-grained tiles (Figure 4(a)), it attempts to isolate non-intersecting  $b \in B$  into smaller tiles while respecting minimum tile dimensions specified by the codec and ensuring that no tile boundary intersects any  $b \in B$ . We evaluate the performance impact of this choice in Section 5.2.2. TASM processes fewer pixels from a video stored with fine-grained tiles because the tiles do not contain the parts of the frame between objects, but it processes more individual tiles because multiple tiles in each frame may contain objects. TASM estimates the overall effectiveness of a layout using a cost function that combines these two metrics, as described in Section 4.1.

In addition to deciding the tile granularity, TASM also chooses *which* objects the tile layout should be designed around. The best choice depends on the queries. For example, if queries target people, a layout around just people, as in Figure 3(d), is more efficient than a layout around both cars and people, as in Figure 3(b). We explain how TASM makes this choice in Section 4.

**3.4.3 Temporally-changing layouts.** Different tile layouts, uniform and non-uniform, can be used throughout a video; the layout can change as often as every GOP. TASM uses different layouts throughout a video to adapt to object locations as they move.

The size of these temporal sections is determined by the *layout duration*, which refers to the number of frames within a SOT. Layout

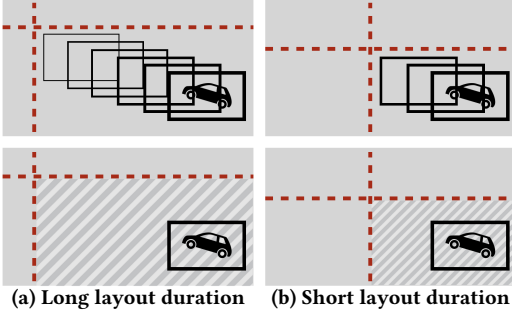


**Figure 5:** (a) shows how more pixels must be decoded on each individual frame when a tile layout extends for many frames compared (b) where fewer frames have the same layout. The boxes show the location of the car on later frames, and the dashed line shows where the frames are divided into tiles. The striped region indicates the tile that would have to be decoded for a query targeting cars.

duration is separate from GOP length; while layout duration cannot be shorter than a GOP, it can extend over multiple GOPs. The layout duration affects the sizes of tiles in non-uniform layouts, as shown in Figure 5. In general, longer tile layout durations lead to larger tiles because TASM must consider more object bounding boxes as objects move and new objects appear, and therefore more data must be decoded on each frame. However, while shorter layout durations lead to more efficient layouts, they also lead to larger storage sizes due to the high storage overhead of changing tile layouts described in Section 2. We evaluate this tradeoff in Figure 9.

**3.4.4 Not tiling.** TASM identifies cases where tiling cannot provide improvement based on the number of pixels the layout enables it to skip. As described in Section 2, the decode cost grows with the number of pixels that are decoded. Layouts that require TASM to decode a similar number of pixels as when the video is not tiled can actually slow queries down due to the implementation complexities that arise from working with multiple tiles. TASM sets a threshold for the minimum reduction in decoding cost that a layout must offer to be considered useful.

**3.4.5 Data storage and retrieval.** TASM stores each tile as a separate video file. For example if a video is encoded with a tile layout of three rows and three columns, TASM stores nine video files, each of which can be decoded individually. Each video acts as a spatial random access point for the region of the frame it contains. If different tile layouts are used in different parts of the video, each tile video contains only the frames with that layout. Figure 1 shows an example of how a video encoded with tiles can be stored using a separate video for every tile. In Figure 1, all of the tiles for frames  $[j + 1, n]$  are stored in the directory `video/frames_j+1-n/` and the upper-left portion of frames  $[j + 1, n]$  are saved in the video `video/frames_j+1-n/tile0.mp4`.

For a query of an object contained within a single tile, TASM retrieves only the relevant tile. For queries over objects spanning multiple tiles, TASM must retrieve and combine the contents of multiple tiles. When a query asks for the entire frame, TASM uses homomorphic stitching to recover the frame as described in Section 2. Because the tiles are stored as standard videos, the system can decode the tiles just like it would any video.

## 4 TILING STRATEGIES

TASM automatically tunes the tile layout of a video to improve query performance. Objects in a video may be *known* or *unknown*. Similarly, workloads or the set of queries presented to a VDBMS may be *known* or *unknown*. When TASM has full knowledge of both the objects targeted by queries and the locations of these objects in video frames, TASM designs tile layouts before queries are processed, as described in Section 4.2. More commonly, the locations of objects are initially unknown and must be incrementally detected as queries are processed. When the types of objects targeted by queries are known, TASM designs tile layouts around these objects as they are detected, as described in Section 4.3. However, when both the objects targeted by queries and their locations are unknown, TASM uses techniques from online indexing to incrementally design layouts based on prior queries and the objects detected so far, as described in Section 4.4.

### 4.1 Notation and cost function

We first introduce notation that will be used throughout this section. A query workload  $Q = \{q_1, \dots, q_n\}$  consists of a set of queries, where each query requests pixels that belong to specified object classes, possibly with additional temporal constraints on the frames the objects must appear in. The set  $O_{q_i}$  represents the set of objects requested by an individual query  $q_i$ . The set  $O_Q = \cup_{q_i \in Q} O_{q_i}$  represents the set of all objects targeted by queries in  $Q$ .

A video  $v = s_0 \oplus \dots \oplus s_n$  is a series of concatenated, non-overlapping, non-empty sequence of tiles (SOTs; see section 2),  $s_i$ . A video layout specification  $\mathcal{L} = s_i \mapsto L$  maps each SOT to a tile layout,  $L$ , which specifies how frames are partitioned into tiles, as described in Section 2. If a SOT is not tiled, then  $s_i \mapsto \omega$ , where  $\omega$  refers to a  $1 \times 1$  tile layout. `PARTITION( $s, O$ )` refers to tiling the SOT using a non-uniform layout around the bounding boxes associated with objects in the set  $O$  using the techniques from Section 3.4.2. For example, `PARTITION( $s, \{car, person\}$ )` refers to creating a layout around cars and people, as in Figure 3(b), while `PARTITION( $s, \{car\}$ )` refers to creating a layout around just cars, as in Figure 3(c).

The estimated cost of executing a query  $q$  over SOT  $s$  encoded with layout  $L$  is  $C(s, q, L) = \beta \cdot P(s, q, L) + \gamma \cdot T(s, q, L)$ .  $C(s, q, L)$  depends on the number of pixels  $P$ , and the number of tiles  $T$  that are decoded, which are both functions of the query and tile layout. To validate this cost function and estimate  $\beta$  and  $\gamma$  to use in experiments, we fit a linear model to the decode times for over 1,400 video, query object, and non-uniform layout combinations used in the microbenchmarks in Section 5.2. The resulting model achieves  $R^2=0.996$ . The exact values of  $\beta$  and  $\gamma$  will depend on the system; TASM can re-estimate them by generating a number of layouts from a small sample of videos and measuring execution time.

TASM uses this cost function to implement a “what-if” interface [12] that estimates the cost of executing queries with alternate layouts. Finally, the cost of executing  $q$  over an entire video  $v$  encoded with layout specification  $\mathcal{L}$  is the sum of its SOT costs (i.e.,  $C(v, q, \mathcal{L}) = \sum_{s_i \in v} C(s_i, q, \mathcal{L}(s_i))$ ) and the cost of executing an entire query workload is the sum over all individual queries,  $C(v, Q, \mathcal{L}) = \sum_{q_i \in Q} C(v, q_i, \mathcal{L})$ .

The difference in estimated query time for query  $q$  over SOT  $s$  between layouts  $L$  and  $L'$  is  $\Delta(q, L, L', s) = C(s, q, L) - C(s, q, L')$ , or simply  $\Delta(q, L, L')$  when  $s$  is obvious from the context. Finally, the cost of (re-)encoding SOT  $s$  with layout  $L$  is  $R(s, L)$ .

## 4.2 Known queries and known objects

We first present TASM’s fundamental video layout optimization assuming a known workload, meaning that TASM knows which objects will be queried in each part of the video, *and* the semantic index contains their locations. These assumptions are unlikely to hold in practice, and we relax them in the following sections.

Given a workload and a complete semantic index, TASM picks tile layouts to minimize execution costs over the entire workload. More formally, the goal is to partition a video into SOTs,  $v = s_0 \oplus \dots \oplus s_n$  and find  $\mathcal{L}^* = \arg \min_{\mathcal{L}} C(v, Q, \mathcal{L})$ .

TASM partitions the video into SOTs at GOP boundaries, so each GOP in the original video corresponds to a SOT in the tiled video. This produces a tiled video with a similar storage cost as the untiled video because it has the same number of keyframes. As mentioned in Section 3.4.3, shorter layout durations lead to greater performance improvements, though they also incur higher storage costs. This tradeoff is shown in Figure 9.

The set of all possible layouts for a given SOT of the video is extremely large; it contains all possible uniform and non-uniform layouts. It would be too computationally expensive for TASM to evaluate every possible layout on every SOT. However, tile layouts that isolate the objects being queried should lead to the greatest performance improvements. Additionally, we empirically demonstrate that non-uniform layouts outperform uniform layouts (see Figure 6(a)), and that fine-grained layouts outperform coarse-grained layouts (see Figure 8). Therefore, for each  $s_i$ , TASM only considers a fine-grained, non-uniform layout around the objects targeted by queries in that SOT,  $O_{s_i} \subseteq O_Q$ . We call this the “known-query/known-object” (KQKO) optimization. The optimization proceeds in two steps. First, for each  $s_i$  and associated layout,  $L = \text{PARTITION}(s_i, O_{s_i})$ , TASM estimates if re-tiling the SOT with  $L$  will improve query performance at all. As described in Section 3.4.4, TASM does not tile  $s_i$  when  $P(s_i, Q, L) > \alpha \cdot P(s_i, Q, \omega)$ , where  $\alpha$  represents the threshold of how much a tile layout must reduce the amount of decoding work. In our experiments we find  $\alpha = 0.8$  to be a good threshold. As shown in Figure 10, this value of  $\alpha$  prevents TASM from picking tile layouts that would slow down query processing, but does not cause TASM to ignore tile layouts that would have significantly sped up query processing. Second, from among all such layouts, TASM selects the layout with the smallest cost for the workload.

## 4.3 Known queries but unknown objects

In many applications, the objects that will be targeted by queries are known, but the locations of these objects in the video are not initially known. For example, if video is collected only to support amber alert applications, then queries will only ask about vehicles. In general, for many applications new video data is appended every time-period and applications tend to query for the same objects over time.

In this scenario, TASM knows  $O_Q$  but not the associated bounding boxes. Once TASM learns the location of the objects, it can directly run the KQKO optimization described in the previous section because it knows that queries will ask about those objects.

We evaluate three possible strategies to learn the object locations and optimize the video file layout on disk:

**Eager detection.** The eager detection strategy consists in running an object detection algorithm (e.g., YOLOv3 [42]) on every frame of a video file to build the semantic index when the video is ingested into the VDBMS. Once the object detector finishes, TASM runs the KQKO optimization using the bounding boxes in the semantic index. The challenge with this strategy is a significant preprocessing overhead before any query executes. This overhead may not pay off if only a small number of queries target certain regions of the video.

**Lazy detection.** In the lazy detection strategy, objects are detected at query time. Instead of initially tiling the entire video, TASM re-encodes SOTs with tiles as it processes queries and learns the locations of objects. After each query, TASM makes tiling decisions based on the objects that have been detected so far. For each SOT, if the semantic index contains the locations of  $O_Q$  in the relevant frames, TASM tiles it using KQKO. If not, TASM waits to tile that SOT because it knows future queries will target objects whose locations are currently unknown, and it cannot be sure whether a particular layout will be beneficial until it knows where those objects are. As shown in Section 5.3, incrementally tiling the video performs well, and can even outperform eagerly tiling the entire video when queries target a subset of the video.

**Edge tiling.** To minimize the overhead of eager object detection, we also explore pushing object detection and tiling to the edge camera that captures the video. The camera leverages its capacity to run object detection on-device to learn the semantic contents of videos even before they arrive at a VDBMS. It can use the object detections to tile the video before it is initially encoded, which avoids the cost of re-encoding the video with tiles once it is ingested into the VDBMS. The VDBMS utilizes the pre-initialized semantic index and pre-tiled video to accelerate even the initial queries over the video. Object detection on cameras may take longer than on more powerful machines, so the challenge lies in generating a sufficient number of high-quality detections to create useful layouts with the limited processing power available to cameras.

In this approach, the VDBMS communicates  $O_Q$  to the camera, which then detects these objects in frames as they are captured and designs tile layouts around their bounding boxes,  $\text{PARTITION}(v, O_Q)$ . The challenge in this approach is the performance of running object detection; background segmentation and cheap object detectors such as Tiny YOLOv3 [42] run quickly, but they produce low-quality identifications which lead to tile layouts that perform poorly, as discussed in Section 5.2.4. In contrast, high-quality object detection models are computationally expensive to run, so cameras may not be able to run the model on every frame; embedded GPUs can run full YOLOv3 at up to 16 fps [20], while videos are commonly captured at rates at or above 30 fps. We find, however, that executing object detection every few frames yields tile layouts that perform similarly to layouts created around detections from every frame, especially when objects within a video are “sparse” (meaning they occupy a small fraction of each frame), as discussed in Section 5.2.4.

#### 4.4 Unknown queries and unknown objects

In general, we expect that both the objects targeted by queries and the locations of these objects will be unknown. In these situations, TASM cannot know how a particular layout will affect the performance of future queries. This is similar to the online indexing problem in relational databases [11] where a system must decide when to build or drop indices without knowing how they will affect future queries. As TASM observes queries and learns the locations of objects, it makes incremental changes to the video’s layout specification. TASM optimizes the layout of each SOT based on the queries that target it. TASM may even tile the same SOT of the video multiple times with different layouts as the semantic index gains more complete information and TASM observes queries that target additional objects. Whereas in Section 4.3 TASM had complete knowledge of  $O_Q$  and therefore no uncertainty about whether it should re-tile a SOT or wait for more objects to be detected, in this scenario TASM must deal with uncertainty when creating layouts because it does not know whether it has seen all of  $O_Q$ , or whether future queries will target new objects.

As TASM re-encodes portions of the video, the video transitions through a series of layout specifications  $\mathcal{L} = [\mathcal{L}_0, \dots, \mathcal{L}_n]$ . For each SOT, its contribution to query time and the cost to re-encode it are independent of other SOTs. This allows TASM to optimize the layout of each SOT independently. For an arbitrary SOT  $s_j$ ,  $\mathbf{L} = [L_0^j, \dots, L_n^j]$  denotes the sequence of layouts it transitions through over the workload.

TASM’s goal is to pick a sequence of layouts for each SOT that minimizes the total execution cost over the workload. Or, for each  $s_j$ , find  $\mathbf{L}^* = \arg \min_{\mathbf{L}} \sum_{q_i \in Q} (C(s_j, q_i, L_i^j) + R(s_j, L_i^j))$ . The first term measures the cost of executing the query over the SOT with its current layout, and the second term measures how expensive it was to transition the SOT to its current layout. If the layout for a SOT does not change between queries (i.e.,  $L_{i-1}^j = L_i^j$ ), then  $R(s_j, L_i^j) = 0$ . However, because future queries are unknown, TASM must pick  $L_{i+1}^j$  for each SOT without knowing  $q_{i+1}$ . Therefore, TASM uses heuristics to pick a sequence of layouts for each SOT,  $\hat{\mathbf{L}}$ , which is hopefully nearly as good as  $\mathbf{L}^*$ .

TASM does not know which objects will be targeted by future queries, but because many applications query for similar objects over time, TASM creates tile layouts optimized for the objects it has seen so far. More formally, let  $O_{Q'}$  be the set of objects TASM has seen in  $Q' = (q_0, \dots, q_i) \subseteq Q$ . When TASM considers layouts for  $L_{i+1}$ , it only considers non-uniform layouts around objects in  $O_{Q'}$ .

However, it is possible that a future query  $q_j$  targets a new class of object:  $O_{q_j} \not\subseteq O_{Q'}$ . While  $L_{i+1}$  will not be optimized for  $O_{q_j}$ , TASM attempts to create layouts that will not hurt the performance of queries for new types of objects. It does this by creating fine-grained tile layouts because, as shown in Figure 8, when queries target objects that were not considered when creating the tile layout ( $\text{PARTITION}(s, O')$ ,  $O' \cap O_{q_j} = \emptyset$ ), fine-grained tiles lead to better query performance than coarse-grained tiles. Objects that are not considered when designing the tile layout may intersect multiple tiles, and it is more efficient for TASM to decode all intersecting tiles when the tiles are small, as in fine-grained layouts, than when the tiles are large, as in coarse-grained layouts.

After executing each query, TASM must decide whether to update the layout of each SOT  $s_j \in v$ . TASM maintains a set of alternative layouts,  $L_{alt} = \{L_0, \dots, L_m\}$ , where each potential layout partitions around a subset of the seen objects that have location information in the semantic index,  $\text{PARTITION}(s_j, O')$ ,  $O' \subseteq O_{Q'}$ . TASM identifies potentially good layouts by estimating the performance improvements that each alternative layout could have provided on queries in  $Q'$ .

As each query executes, TASM accumulates regret [13]  $\delta_k^j$  for each  $s_j$  and alternative layout  $L_k$ , which measures the total estimated performance improvement over the query history. After each  $q_i$ , TASM estimates  $\forall s_j \in v, L_k \in L_{alt}, \delta_k^j = \delta_k^j + \Delta(q_i, L_i^j, L_k)$ , where initially each  $\delta_k^j = 0$  when the first query is executed.  $\Delta(q_i, L_i^j, L_k)$  measures the estimated performance improvement of executing the query on  $s_j$  with an alternative layout rather than its current layout,  $L_i^j$ , using the cost function described in Section 4.1.

As an example, consider the amber alert application from Section 1. Initially the traffic video is un-tiled, so for each  $s_i$ ,  $\mathcal{L}(s_i) = \omega$ . Suppose the first query is for cars in  $s_0$ . TASM updates  $L_{alt} = \{\{car\}\}$  to consider layouts around cars. TASM accumulates regret for  $s_0$  as  $\delta_{car}^0 = \Delta(q_0, \omega, \text{PARTITION}(s_0, \{car\}))$ , and the regret is positive because tiling around cars would accelerate the query. Suppose the next query is for people in  $s_0$ . TASM updates  $L_{alt} = \{\{car\}, \{person\}, \{car, person\}\}$  to consider layouts around cars and people. The regret for  $\text{PARTITION}(s_0, \{car\})$  on  $q_1$  will likely be negative because layouts around anything other than the query object tend to perform poorly (see Figure 8(b)), so the value of  $\delta_{car}^0$  will decrease slightly. TASM retroactively accumulates regret for the two new layouts. The accumulated regret for  $\text{PARTITION}(s_0, \{person\})$  will be similar to  $\delta_{car}^0$  because it would accelerate  $q_1$  and likely hurt  $q_0$ .  $\text{PARTITION}(s_0, \{car, person\})$  accumulates positive regret from both  $q_0$  and  $q_1$ , so after both queries it has the largest accumulated regret.

In addition to considering the performance improvements offered by alternative layouts, TASM must consider the cost of transitioning  $s_j$  to a new layout; it estimates the cost of  $R(s_j, L_k)$  based on the encoding performance of the system. TASM re-tiles  $s_j$  with  $L_k$  when  $\delta_k^j > \eta \cdot R(s_j, L_k)$ . The value of  $\eta$  determines how quickly TASM re-tiles the video after observing queries for different objects. Using  $\eta = 0$  risks wasting resources to re-tile SOTs. The work to re-tile could be wasted if a SOT is never queried again because no queries will experience an improved performance from the tiled layout. The work to re-tile can also be wasted if queries target different objects because TASM will re-tile after each query with layouts optimized for just that query. Values of  $\eta > 0$  enable TASM to observe multiple queries before picking layouts, so the layouts can be optimized for multiple types of objects. Observing multiple queries before committing to re-tiling also enables TASM to avoid creating layouts optimized for objects that are infrequently queried because layouts around more representative objects will accumulate more regret. However, if the value of  $\eta$  is too large, it reduces the number of queries whose performance benefits from the tiled layout. Using a value of  $\eta = 1$  is similar to the logic used in the online indexing algorithm in [11], and we find it generally works well in this scenario, as shown in Figure 11.

**Table 1: Video datasets**

Video set	Type	Duration (sec.)	Res.	Per-frame object coverage (%)	Frequently occurring objects
Visual Road [18]	Synth.	540–900	2K, 4K	0.06–10	car, person
Netflix public [30]	Real	6	2K	0.32–49	person, car, bird
Netflix Open Source [43]	Real, Synth.	720	2K, 4K	25–45	person, car, sheep
XIPH [5]	Real	4–20	2K, 4K	2–59	car, person, boat
MOT16 [35]	Real	15–30	2K	3–36	car, person
El Fuente [29]	Real	480 (full) 15–45 (scenes)	4K	1–47	person, car, boat, bicycle

## 5 EVALUATION

We have implemented a prototype of TASM in C++ as an extension to LightDB [17]. Video encoding and decoding are implemented using NVENCODE/NVDECODER [38] with the HEVC codec. All experiments are performed on a single node running Ubuntu 16.04 containing an Intel i7-6800K processor (3.4 GHz, 6 cores), and a Nvidia P5000 GPU with two NVENCODER chipsets. Our prototype does not parallelize encoding or decoding multiple tiles at once. FFmpeg [10] is used to measure the quality of the videos.

We evaluate TASM on both real and synthetic videos with a variety of resolutions and contents as shown in Table 1. We do not evaluate on lower-resolution videos (i.e., <2K) because we found that decoding low-resolution video did not exhibit significant overhead. In addition to evaluating the full El Fuente video, we also manually decompose it into its individual scenes using the scene boundaries specified in [29] and evaluate each independently. All experiments rely on YOLOv3 [42] to detect objects within videos and populate the semantic index, except for the MOT16 videos where we use the object detections from the dataset [35]. We use SQLite [6] to store semantically indexed data, and our prototype maps bounding boxes to tiles at query time, though a future enhancement involves pre-computing and storing this mapping in the index.

The queries used in the microbenchmarks evaluated in Section 5.2 are simple selections of the form “SELECT o FROM v”, which cause TASM to decode all pixels belonging to the specified object class o in video v. The queries used to evaluate tiling over workloads in Section 5.3 additionally include a temporal predicate (i.e., “SELECT o FROM v WHERE start < t < end”). Reported query times include both the index look-up time to determine which tiles must be processed and the time to decode the tiles.

Unless otherwise specified, queries target the most frequently occurring object classes in each video. Some videos primarily show a single type of object (e.g., some Netflix public dataset [30] videos show only people or birds), in which case queries over that video target just that object. Other videos feature multiple types of objects with similar frequency (e.g., the Visual Road [18] videos show similar numbers of cars and pedestrians), in which case we evaluate on queries that target each object type. Queries over the MOT16 videos retrieve cars *and* pedestrians because the bounding boxes that come with the dataset [35] are unlabeled, so we store them in the semantic index with a generic label of “object”. For all graphs, the bars show median value, while the error bars denote interquartile range (IQR).

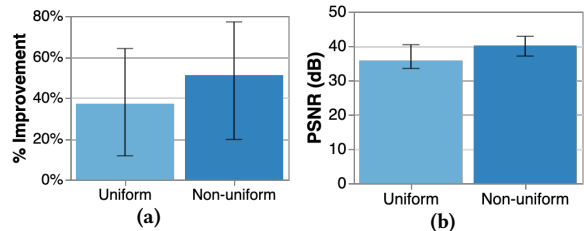


**Figure 6: (a) shows the improvement in query time achieved by tiling the video using the fastest uniform and non-uniform layout for each video and query object. (b) shows the quality of these layouts compared to the untiled video.**

### 5.1 Tiling effect on decode cost and quality

We first evaluate whether tiling can provide meaningful improvements in query time without degrading the visual quality of videos. Figure 6(a) shows the improvement in query time achieved by tiling videos compared to executing queries over a video that is not tiled. For each video and query object, the uniform and non-uniform layouts are hand-picked to be those that empirically led to the greatest performance improvement. Figure 6 only shows the median and interquartile range for videos and objects that benefit from tiling. We discuss how TASM determines whether to tile a video or not in Section 5.2.3 and how TASM selects the optimal tile layout in Section 5.2 and Section 5.3.

Figure 6(a) shows that tiling a video can speed up queries, and non-uniform layouts tend to lead to greater performance improvements compared to uniform layouts. Over all videos and query objects, the best uniform layout gives an average of 37% improvement in decode time, and the best non-uniform layout gives an average of 51% improvement. For a given video and query object, a non-uniform layout provides an average of 10% improvement and up to a 35% improvement over the best uniform layout.

Figure 6(b) shows that tiling maintains good visual quality in videos. Peak signal-to-noise ratio (PSNR) values above 30 dB indicate acceptable visual quality [31], while videos with PSNR values  $\geq 40$  dB are perceived to have good quality [30, 45, 46]. PSNR was computed over the entire tiled video stitched using homomorphic stitching [17] and compared against the original, untiled video. Videos tiled with the best uniform layout have an average PSNR of 36 dB, and videos tiled with the best non-uniform layout have an average PSNR of 40 dB. PSNR is likely lower for the uniform layouts because the uniform layouts with the greatest improvement have many tiles (the median number of tiles is 25), and therefore a large number of tile boundaries where quality is degraded. For comparison, the median PSNR of the videos after re-encoding them without tiles is 46 dB.

### 5.2 Microbenchmarks

**5.2.1 Uniform tiles.** We dig deeper into the results of Figure 6 and show in Figure 7 the performance improvements achieved by varying the number of uniform tiles on the same set of videos. Figure 7 shows that creating more uniform tiles initially improves query time because tiles contain fewer non-object pixels; average improvement increases from 19% with a  $2 \times 2$  uniform layout to 36% with a  $5 \times 5$  layout. However, as the number of tiles grows, the per-tile decode overhead begins to slow queries down; the average

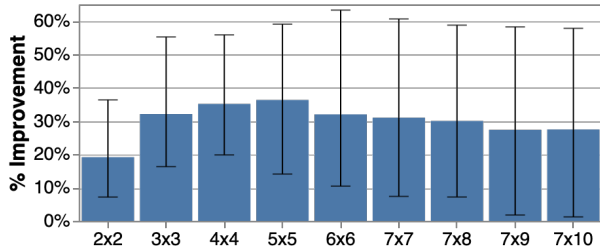


Figure 7: This figure shows improvement in query time achieved with various uniform layouts compared to the untiled video.

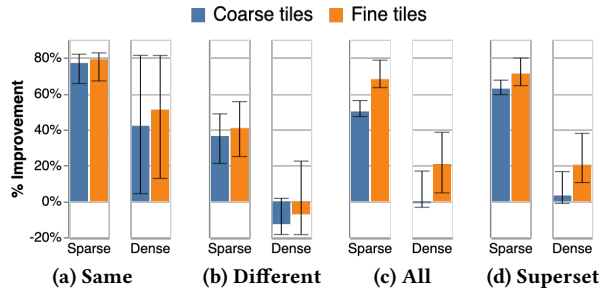


Figure 8: This plot shows the effect of tile granularity on query time compared to untiled videos. All videos used a one second tile layout duration. In “sparse” videos, detected objects take up less than 20% of each frame on average, while in “dense” videos they take up at least 20%.

improvement for a 7×10 layout is 28%. Additionally, the variation in performance across videos and query objects increases with the number of tiles, as indicated by the widening of the IQR bars. For example, the interquartile range for a 7×10 layout ranges from 1% to 58%. This demonstrates that the same uniform tile layout does not work equally well on all videos and query objects.

**5.2.2 Non-uniform tiles.** The performance of non-uniform tile layouts depends on which objects are targeted by queries and which objects are considered when designing the tile layout. Figure 8 shows the results from different settings. We classify layouts as *same*, *different*, *all*, or *superset*. “Same” describes a tile layout around the query object. “Different” describes a layout around an object different from the query object (e.g., tiling around people but querying for cars). “All” describes tiling around *all* objects detected in the video. Finally, “superset” evaluates what happens if we tile around the target object and only 1-2 other, frequently occurring objects (e.g., tiling around the locations of cars *and* people, as in in Figure 3(b)). We further classify videos as either *sparse*, where the average area occupied by all objects in a frame is < 20%, or *dense*, where the average area occupied by all objects is ≥ 20%. Figure 8 shows the results. In this experiment, we only show data points for Visual Road videos and El Fuente scenes, which feature multiple types of objects to be used in the “different” and “superset” categories; the other videos primarily feature a single type of object.

Figure 8 shows that, in general, sparse videos achieve larger improvements with tiling than dense videos, and tile granularity has a larger impact on performance in videos when objects are dense. Figure 8(a) shows that when the tile layout is constructed around the query object, tile granularity does not have a large impact on

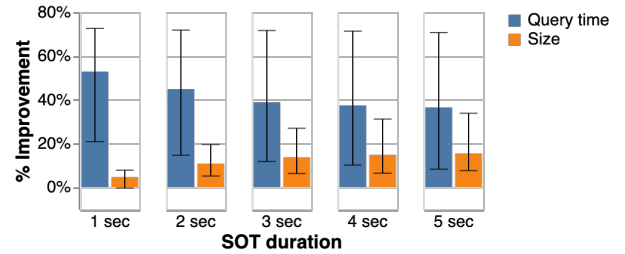


Figure 9: This plot shows the effect of SOT duration on query time and storage cost. Tiled videos were encoded with fine-grained tiles and a GOP length equal to the SOT duration.

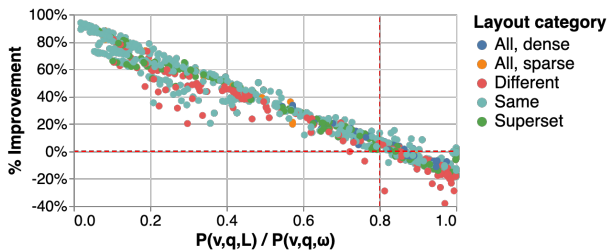
query performance. The average improvement for fine-grained tiles is 79% and 51% for sparse and dense videos, respectively. It drops to 77% and 42% for coarse-grained tiles.

Figure 8(b) shows that tiling around an object other than the query object can hurt performance when objects are dense. This happens when one object class has a higher density than others, meaning it occupies more area on each frame. Querying for the dense object using a layout around the sparse object requires TASM to decode most of the tiles because the dense object occupies much of each frame. Querying for a sparse object using a layout designed for a different object, although the query object may intersect multiple tiles, TASM can still reduce the work it performs if the tiles are small. Performance improvement at both granularities suffers when the object types do not appear on the same frames.

Figure 8(c) shows that tiling around all detected objects can be an effective strategy when objects do not appear in much of the frame; the median improvement for sparse videos is 68% for fine-grained tiles, and 50% for coarse-grained tiles. However, when objects appear in most parts of the frame, tiling around all objects is *not* generally effective. Median improvement for fine-grained tiles is 21%, and it is 1% *worse* for coarse-grained tiles. Figure 8(d) shows that the “superset” strategy performs similarly to tiling around all objects; considering only two or three types of objects rather than all objects when generating layouts leads to small performance gains.

These results demonstrate that tiling around an object (or objects) other than the query object slows queries down compared to tiling around the query object. However, using fine-grained tiles in these cases can still lead to moderate performance improvements. Fine-grained tiles are smaller, so they enable decoding fewer non-object pixels even when the tiles are not designed around the query object.

**Sequence of tiles (SOT) duration.** Here we evaluate the impact of SOT duration (the number of frames with the same tile layout) on the performance of non-uniform tile layouts. SOT duration affects both the sizes of tiles as well as the size of the video. Layout changes must happen at GOP boundaries, so short SOTs require short GOPs and lead to larger storage sizes (see Section 2).



**Figure 10:** This figure plots the ratio of the number of pixels decoded with a non-uniform layout to the number of pixels decoded with no tiles ( $P(v, q, L)/P(v, q, \omega)$ ) vs. performance improvement. Each point represents a video, query object, and non-uniform layout. Points below the horizontal dashed line at 0% represent cases where queries ran more slowly on the tiled video. Points to the right of the vertical dashed line at 0.8 represent videos that would not be tiled when the threshold for tiling is  $P(v, q, L)/P(v, q, \omega) < 0.8$ .

Figure 9 shows the effect of SOT duration on query performance and storage size. The tiled videos are encoded with a GOP length equal to the SOT duration. We compare query performance and storage size to an untiled video encoded with one-second GOPs (the default GOP duration in most video encoders). Shorter SOT durations lead to larger improvements in query performance because the tiles are smaller and contain fewer non-object pixels. The average improvement in query performance decreases from 53% for one-second SOT durations to 36% for five-second SOT durations. However, shorter SOTs also lead to larger storage costs compared to videos encoded with longer SOTs because there are more keyframes. Videos encoded with one-second SOTs have an average of 5% smaller storage size than the original video, while videos encoded with five-second SOTs are on average 15% smaller than the original video. Note that we see a small improvement in the size of the one-second non-uniform layout when compared to the original video (also encoded with one-second GOPs); this is due to video encoders being inherently lossy and having the ability to exploit additional compression opportunities during recompression. None of the videos we evaluate on contain prolonged static scenes. If that were the case, we expect SOT duration would not have a large impact on performance.

**5.2.3 Not tiling.** There are videos where tiling is an ineffective strategy to improve query performance. To identify cases where tiling should not be used, we evaluate the effectiveness of a decision rule based on the number of pixels decoded with a given layout.

Figure 10 plots the improvement in query time against the ratio of pixels decoded with a non-uniform layout compared to the untiled video (i.e.,  $P(v, q, L)/P(v, q, \omega)$ ) for various videos and query objects. Using a threshold of not tiling when  $P(v, q, L)/P(v, q, \omega) > 0.8$  captures nearly all tile layouts that slow queries down (i.e., the improvement is negative). A small number of videos achieve performance improvements with a non-uniform layout even when  $P(v, q, L)/P(v, q, \omega) > 0.8$  (the points in the upper-right quadrant of Figure 10), however, the performance improvement offered by these layouts is small,  $< 20\%$ .

**5.2.4 Tile layouts based on cheap object detection.** To evaluate the potential of creating tile layouts for videos on edge devices, we measure the effectiveness of layouts created around objects detected with cheaper methods than running YOLOv3 per frame. We first try KNN-based background segmentation implemented in OpenCV [39] but find it does not accurately detect the correct foreground pixels, especially when the camera moves. Additionally, objects being queried will occasionally be in the background of a video. Tile layouts created around the detected foreground pixels perform on average 3% worse than not tiling the video. We then try using YOLOv3-tiny which runs more quickly than full YOLOv3, but is less accurate. We find the lower accuracy leads to inefficient tile layouts because only a small number of objects are detected; the median improvement achieved by layouts around all objects detected by YOLOv3-tiny is just 16%.

Finally, we measure the effectiveness of creating tile layouts around objects detected by full YOLOv3 run every five frames. This technique is viable because objects generally appear in multiple frames, so running the object detector every few frames still captures the motion of objects. Importantly, running the more complex model every few frames is feasible on certain edge configurations; current embedded GPUs can achieve up to 16 FPS on full YOLOv3 [20]. Fine-grained layouts created around all objects detected every five frames perform similarly to layouts around all objects detected every frame (i.e., the results in Figure 8(c)). Detecting objects every five frames in sparse videos has a median improvement of 63%, which is 5% worse than doing so every frame. The median improvement in dense videos is 5%, which is 16% worse than doing so every frame.

### 5.3 Incremental tiling

In this section, we evaluate strategies for tiling videos over various query workloads. We construct the workloads to represent possible query patterns over videos. The baseline strategies are not tiling the video (“Not tiled”) and tiling the video around all detected objects before queries are processed (“All objects”). We compare these baselines against two incremental tiling strategies. The first incremental strategy re-tiles GOPs after observing a query for a new object type (“Incremental, more”). It re-tiles each GOP with a non-uniform, fine-grained layout around all the object classes that have been queried so far. For example, if a GOP is queried for cars, TASM would tile that GOP around cars. If the next query is for people, TASM would re-tile the GOP around cars and people. The final strategy we evaluate is the regret-based approach from Section 4.4 (“Incremental, regret”). In this strategy, TASM keeps track of alternative layouts based on the objects that have been queried for so far, and it re-tiles GOPs once the regret for a particular layout exceeds the estimated re-encoding cost if TASM estimates the layout will not hurt performance.

TASM estimates the layout will hurt performance if, for any query,  $P(s_i, q_i, L) \geq \alpha \cdot P(s_i, q_i, \omega)$ , where  $\alpha = 0.8$  is chosen based on our results from Section 5.2.3. TASM estimates the regret using the cost function described in Section 4.1. Similarly, the re-encoding cost is estimated using a linear model based on the number of pixels being encoded. It was fit based on the time to encode videos with the various layouts used in the microbenchmarks.

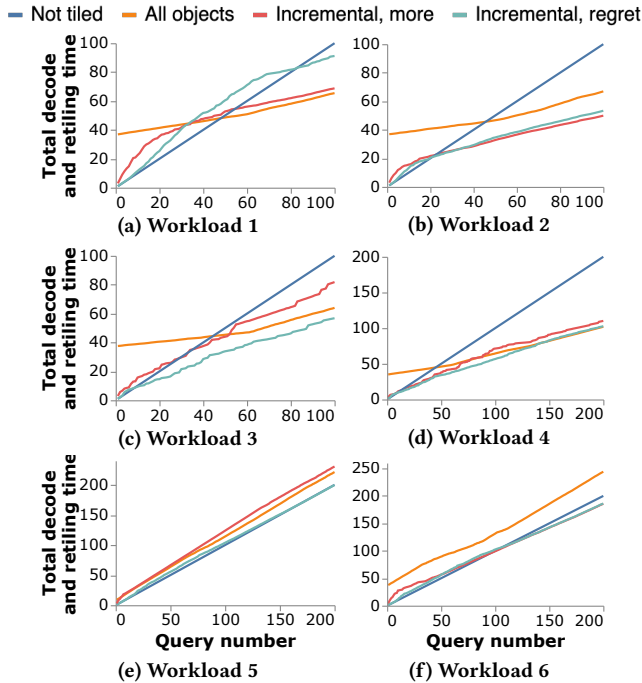


**Figure 11: Cumulative decode and re-tiling time for various strategies and workloads. All values are normalized to the time to execute each query over the untilted videos.**

**Table 2: Cumulative workload time. All values are normalized to the time to execute each query over the untilted videos.**

Workload	Not tiled	All objects			Incremental, more			Incremental, regret		
		25%	50%	75%	25%	50%	75%	25%	50%	75%
W1	100	60	65	75	62	69	71	88	91	96
W2	100	59	67	70	40	50	57	42	53	60
W3	100	62	64	65	74	82	85	54	57	67
W4	200	81	102	111	101	110	121	100	103	124
W5	200	205	221	238	192	230	249	187	200	214
W6	200	203	244	261	135	186	250	147	186	219

All plots show the cumulative decode and re-tiling time normalized to the time to execute the queries on the untilted video. The decode time refers to the time spent decoding the pixels requested by each query. The re-tiling time is the time spent re-encoding the video with new layouts. The time to initially tile the video around all objects is included with the first query for the “all objects” strategy. For each plot in Figure 11, the line shows the median over all videos the workload was evaluated on. Table 2 contains the interquartile range across all videos in each workload. The first four workloads are evaluated on Visual Road videos where tiling around all objects performs well because objects are sparse. The last two workloads are evaluated on videos and scenes with dense objects, so tiling around all objects does not perform well.

We first evaluate Workload 1, a simple workload where each query targets the same object class, and queries are uniformly

distributed over the entire video. The workload consists of 100 one-minute queries for cars over each Visual Road video. The start frames of each query are picked according to a uniform distribution over the entire video. As shown in Figure 11(a), when queries are uniformly distributed over the video, pre-tiling around all objects performs well. Incrementally tiling without regret also performs well because only a single object is ever queried for, so SOTs are re-tiled to a layout that speeds up future queries. Incrementally tiling with regret leads to poor performance, at least over a small number of queries, because TASM must observe multiple queries over the same SOT before enough regret accumulates to re-tile it. This requires many total queries to be executed when they are uniformly distributed over the entire video.

We next evaluate Workload 2, which examines the performance when queries are restricted to a subset of the video. Workload 2 also consists of 100 one-minute queries over the Visual Road videos. Each query has a 50% chance of being for cars or people. The queries are restricted to frames in the first 25% of the video. As shown in Figure 11(b), both incremental strategies perform similarly well, and they both perform better than pre-tiling the entire video around all objects. Encoding the entire video with tiles is wasteful when only a small portion of the video is ever queried.

Workload 3 measures the performance when queries are biased towards one section of a video, and while the queries generally target the same object classes, a minority of queries target a less-common object class. The workload consists of 100 queries over the Visual Road videos, where each query has a 47.5% chance of being for cars, a 47.5% chance of being for people, and a 5% chance of being for traffic lights. The workload excludes one 4K video that did not contain any traffic lights. The start frame of each query is picked according to a Zipfian distribution, so queries are more likely to target frames at the beginning of the video. As shown in Figure 11(c), incrementally tiling with the regret-based approach performs better than incrementally tiling around more objects because it is less likely to spend time re-tiling sections of the video with tile layouts designed around the object that is rarely queried for.

Workload 4 measures performance when queries target different objects over time. It consists of 200 one-minute queries over the Visual Road videos, where the first third of queries are for cars, the middle third of queries are for people, and the final third of queries are for cars. The start frames of the queries are picked following a Zipfian distribution. As shown in Figure 11(d), the incremental, regret-based approach performs well and does not have any large jumps in decode and re-tiling time when the query object changes.

Workload 5 measures the performance of the various strategies when tiling does not help performance. It is evaluated on select videos from the Xiph [5], Netflix public dataset [30], and scenes from the full El Fuente video [29] that contain diverse scenes with many types of objects (e.g., markets filled people, parked cars, and different kinds of food). The start frames of queries are picked following a uniform distribution, and each query targets a one-second segment. Queries are randomly picked for one of the primary objects classes in the scene. As shown in Figure 11(e), only the incremental, regret-based approach is able to keep costs similar to the not-tiled case. Tiling around all objects leads to poor performance because objects are dense in these scenes. Additionally, the “incremental, more” approach leads to poor performance

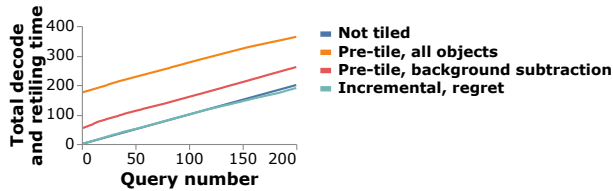


**Figure 12: Cumulative decode and re-tiling time, including initial detection costs. All values are normalized to the time to execute each query over the untilted videos.**

because it spends time re-tiling portions of the video with layouts that lead to similar performance as the untilted video.

Finally, Workload 6 measures the performance of the various strategies when tiling around the query object can improve performance, but tiling around all objects hurts performance. It is evaluated on select videos from the Netflix public dataset [30] and scenes from the full El Fuente video [29] where tiling around one object performs well, but tiling around all objects performs poorly. The start frames of queries are picked following a uniform distribution, and each query targets a one-second segment. Each query targets the same object class. As shown in Figure 11(f), both incremental strategies eventually achieve layouts that perform better than not tiling the video. Pre-tiling the video around all objects performs poorly because objects in these videos are dense.

Initially tiling the video has high upfront costs both in detecting objects and in tiling the video. Figure 12 shows the costs of evaluating Workload 5, but it includes the initial detection time for strategies that tile the video before queries are executed. The initial cost of the “pre-tiling, all objects” strategy includes the cost of running object detection over the videos using YOLOv3 on the GPU and tiling the videos around all detected objects. The initial cost of the “pre-tiling, background subtraction” strategy includes the cost of running KNN-based background subtraction over the video using OpenCV [39] and tiling the videos around all detected foreground pixels. As the workload progresses, both strategies use the incremental, regret-based approach to incrementally modify the initial layouts. The “incremental, regret” strategy does not do any upfront work, but incrementally tiles portions of the video as queries execute. Figure 12 shows that the high upfront cost of running object detection or background subtraction does not amortize, even after 200 queries. This motivates pushing detection to the camera, if possible.

## 6 RELATED WORK

TASM focuses on optimizing query execution at the storage layer, while many recent VDBMSs accelerate queries using other techniques. Systems like Blazeflt [27] and NoScope [28] apply specialized neural networks that run more quickly than general object detectors. Focus [22] shifts some processing to ingest-time. Other systems prioritize evaluating expensive models on promising frames: probabilistic predicates [33] and ExSample [36] use statistical techniques, MIRIS [9] uses sampling, and SVQ [51] uses deep learning filters. Information about the semantic content of videos generated by these systems could be incorporated into TASM’s semantic index to inform tiling decisions. Systems such as LightDB [17], Optasia [32], and Scanner [40] already

accelerate queries through parallelization and deduplication of work, while systems like VideoEdge [23] distribute processing over clusters. These general VDBMSs could incorporate TASM to further accelerate query processing. Systems such as Panorama [54] and Recall [14] expand the set of queries that can be executed over videos, which is orthogonal to how the videos are stored.

Recent systems also focus on optimizing the storage of videos. VStore [52] finds the optimal encoding parameters for videos to increase processing speed while maintaining accuracy in downstream analyses. It improves performance by reducing the quality of the video, while TASM attempts to maintain video quality. Additionally, VStore must profile all downstream operators to determine the encoding parameters, while TASM can work incrementally as queries are processed. Vignette [34] uses tiles to optimize video storage for perception-based compression, but only considers uniform layouts.

TASM’s incremental tiling approach is similar to database cracking [15, 24], which incrementally reorganizes the section of data processed by each query, and online indexing [11] which creates and modifies indices as queries are processed. Regret has also been used to design economic model self-tuning indices and caches in a shared cloud database [13]. TASM extends these relational storage techniques to provide efficient access to video data.

TASM proposes utilizing the improving compute capacity of edge devices to generate the semantic index and tile layouts on-camera. Achieving real-time object detection on resource-limited edge devices is an active area of research. Systems like MARLIN [8] speed up object detection on-device by combining expensive object detection with cheap object tracking methods. Alternative approaches distribute computation between the edge device and cloud, like MCDNN [16], Rocket [7], and DeepDecision [41], or use smaller models to provide faster inference on the edge, such as MobileNets [21] and YOLOv3-tiny [42].

Finally, the idea of a “semantic index” has been proposed in the context of applying latent semantic analysis to images [19]. The semantic index used by TASM is unrelated to the field of latent semantic analysis which focuses on the semantic intent of queries.

The observation that the flexibility to retrieve spatial subsets of videos is useful has come up in other application domains. For video streaming applications, the MPEG DASH SRD standard [37] is motivated by a similar observation that occasionally just a spatial subset of videos is requested by streaming clients. While it specifies a model to support streaming spatial subsets of video to clients, it does not specify *how* to efficiently partition videos into tiles.

## 7 CONCLUSION

This paper introduces the design of TASM, a tile-based storage manager, which designs tile layouts that improve query performance by incorporating information about the semantic content of the video along with observations about which objects are targeted by queries. TASM uses a semantic index in conjunction with the video codec feature of tiles to optimize the storage of videos for queries that retrieve subsets of pixels within frames. We propose strategies that allow TASM to incrementally tile sections of the video as queries are executed and detect objects and demonstrate that these strategies lead to improved performance.

## 8 ACKNOWLEDGEMENTS

This work is supported by the National Science Foundation through NSF grant CCF-1703051, an award from the University of Washington Reality Lab; and a gift from Intel. This work is supported in part by the National Science Foundation through grants IIS-1546083, IIS-2027575, and DOE award DE-SC0016260; the Intel-NSF CAPA center, and gifts from Adobe and Facebook.

## REFERENCES

- [1] 2019. *Advanced video coding for generic audiovisual services*. Rec. ITU-T H.264 and ISO/IEC 14496-10.
- [2] 2019. AV1 Bitstream & Decoding Process Specification. <https://aomediacodec.github.io/av1-spec/av1-spec.pdf>.
- [3] 2019. Bosch Camera Trainer with FW 7.10 and CM 6.20. <https://www.boschsecurity.com/us/en/solutions/video-systems/video-analytics/technical-documentation-for-video-analytics/>. Accessed: 2020-06-11.
- [4] 2019. *High Efficiency Video Coding*. Rec. ITU-T H.265 and ISO/IEC 23008-2.
- [5] 2019. Xiph.org Video Test Media. <https://media.xiph.org/video/derf/>. Accessed: 2020-06-01.
- [6] 2020. SQLite. <https://sqlite.org/index.html>.
- [7] Ganesh Ananthanarayanan, Paramvir Bahl, Peter Bodik, Krishna Chintalapudi, Matthai Philipose, Lenin Ravindranath, and Sudipta Sinha. 2017. Real-Time Video Analytics: The Killer App for Edge Computing. *IEEE Computer* 50, 10 (2017), 58–67.
- [8] Kittipat Apicharttrisor, Xukan Ran, Jiayi Chen, Srikanth V. Krishnamurthy, and Amit K. Roy-Chowdhury. 2019. Frugal following: power thrifty object detection and tracking for mobile augmented reality. In *SensSys*. ACM, 96–109.
- [9] Favven Bastani, Songtao He, Arjun Balasingam, Karthik Gopalakrishnan, Mohammad Alizadeh, Hari Balakrishnan, Michael J. Cafarella, Tim Kraska, and Sam Madden. 2020. MIRIS: Fast Object Track Queries in Video. In *SIGMOD*. ACM, To appear.
- [10] Fabrice Bellard. 2018. Ffmpeg. <https://ffmpeg.org>.
- [11] Nicolas Bruno and Surajit Chaudhuri. 2007. An Online Approach to Physical Design Tuning. In *ICDE*, Rada Chirkova, Asuman Dogac, M. Tamer Özsu, and Timos K. Sellis (Eds.). IEEE Computer Society, 826–835.
- [12] Surajit Chaudhuri and Vivek R. Narasayya. 1998. AutoAdmin ‘What-if’ Index Analysis Utility. In *SIGMOD*. ACM Press, 367–378.
- [13] Debabrata Dash, Verena Kantere, and Anastasia Ailamaki. 2009. An Economic Model for Self-Tuned Cloud Caching. In *ICDE*. IEEE Computer Society, 1687–1693.
- [14] Daniel Y. Fu, Will Crichton, James Hong, Xinwei Yao, Haotian Zhang, Anh Truong, Avnika Narayan, Maneesh Agrawala, Christopher Ré, and Kayvon Fatahalian. 2019. ReCall: Specifying Video Events using Compositions of Spatiotemporal Labels. *CoRR* abs/1910.02993 (2019).
- [15] Felix Halim, Stratos Idreos, Panagiotis Karras, and Roland H. C. Yap. 2012. Stochastic Database Cracking: Towards Robust Adaptive Indexing in Main-Memory Column-Stores. *PVLDB* 5, 6 (2012), 502–513.
- [16] Seungyeop Han, Haichen Shen, Matthai Philipose, Sharad Agarwal, Alec Wolman, and Arvind Krishnamurthy. 2016. MCDNN: An Approximation-Based Execution Framework for Deep Stream Processing Under Resource Constraints. In *MobiSys*. ACM, 123–136.
- [17] Brandon Haynes, Amrita Mazumdar, Armin Alaghi, Magdalena Balazinska, Luis Ceze, and Alvin Cheung. 2018. LightDB: A DBMS for Virtual Reality Video. *PVLDB* 11, 10 (2018), 1192–1205.
- [18] Brandon Haynes, Amrita Mazumdar, Magdalena Balazinska, Luis Ceze, and Alvin Cheung. 2019. Visual Road: A Video Data Management Benchmark. In *SIGMOD*. ACM, 972–987.
- [19] Douglas R. Heisterkamp. 2002. Building a Latent Semantic Index of an Image Database from Patterns of Relevance Feedback. In *ICPR (4)*. IEEE Computer Society, 134–137.
- [20] Sabir Hossain and Deok-Jin Lee. 2019. Deep Learning-Based Real-Time Multiple-Object Detection and Tracking from Aerial Imagery via a Flying Robot with GPU-Based Embedded Devices. *Sensors* 19, 15 (2019), 3371.
- [21] Andrew G. Howard, Menglong Zhu, Bo Chen, Dmitry Kalenichenko, Weijun Wang, Tobias Weyand, Marco Andreetto, and Hartwig Adam. 2017. MobileNets: Efficient Convolutional Neural Networks for Mobile Vision Applications. *CoRR* abs/1704.04861 (2017).
- [22] Kevin Hsieh, Ganesh Ananthanarayanan, Peter Bodik, Shivaram Venkataraman, Paramvir Bahl, Matthai Philipose, Phillip B. Gibbons, and Onur Mutlu. 2018. Focus: Querying Large Video Datasets with Low Latency and Low Cost. In *OSDI*. USENIX Association, 269–286.
- [23] Chien-Chun Hung, Ganesh Ananthanarayanan, Peter Bodik, Leana Golubchik, Minlan Yu, Paramvir Bahl, and Matthai Philipose. 2018. VideoEdge: Processing Camera Streams using Hierarchical Clusters. In *SEC*. IEEE, 115–131.
- [24] Stratos Idreos, Martin L. Kersten, and Stefan Manegold. 2007. Database Cracking. In *CIDR*. [www.cidrdb.org](http://www.cidrdb.org), 68–78.
- [25] Junchen Jiang, Ganesh Ananthanarayanan, Peter Bodik, Siddhartha Sen, and Ion Stoica. 2018. Chameleon: scalable adaptation of video analytics. In *SIGCOMM*. 253–266.
- [26] Daniel Kang, Peter Bailis, and Matei Zaharia. 2018. BlazeIt: Fast Exploratory Video Queries using Neural Networks. *CoRR* abs/1805.01046 (2018).
- [27] Daniel Kang, Peter Bailis, and Matei Zaharia. 2019. BlazeIt: Optimizing Declarative Aggregation and Limit Queries for Neural Network-Based Video Analytics. *PVLDB* 13, 4 (2019), 533–546.
- [28] Daniel Kang, John Emmons, Firas Abuzaid, Peter Bailis, and Matei Zaharia. 2017. NoScope: Optimizing Deep CNN-Based Queries over Video Streams at Scale. *PVLDB* 10, 11 (2017), 1586–1597.
- [29] Ioannis Katsavounidis. [n.d.]. NETFLIX ÅÅÅ “El Fuente” video sequence details and scenes. [https://www.cdvl.org/documents/ElFuente\\_summary.pdf](https://www.cdvl.org/documents/ElFuente_summary.pdf). Accessed: 2020-06-01.
- [30] Zhi Li, Anne Aaron, Ioannis Katsavounidis, Anush Moorthy, and Megha Manohara. 2016. Toward A Practical Perceptual Video Quality Metric. <https://netflixtechblog.com/toward-a-practical-perceptual-video-quality-metric-653f208b9652>. Accessed: 2020-06-01.
- [31] Andrea Lottarini, Alex Ramirez, Joel Coburn, Martha A. Kim, Parthasarathy Ranganathan, Daniel Stodolsky, and Mark Wachsler. 2018. vbench: Benchmarking Video Transcoding in the Cloud. In *ASPLOS*. ACM, 797–809.
- [32] Yao Lu, Aakanksha Chowdhery, and Srikanth Kandula. 2016. Optasia: A Relational Platform for Efficient Large-Scale Video Analytics. In *SoCC*. ACM, 57–70.
- [33] Yao Lu, Aakanksha Chowdhery, Srikanth Kandula, and Surajit Chaudhuri. 2018. Accelerating Machine Learning Inference with Probabilistic Predicates. In *SIGMOD*. ACM, 1493–1508.
- [34] Amrita Mazumdar, Brandon Haynes, Magda Balazinska, Luis Ceze, Alvin Cheung, and Mark Oskin. 2019. Perceptual Compression for Video Storage and Processing Systems. In *SoCC*. ACM, 179–192.
- [35] Anton Milan, Laura Leal-Taixé, Ian D. Reid, Stefan Roth, and Konrad Schindler. 2016. MOT16: A Benchmark for Multi-Object Tracking. *CoRR* abs/1603.00831 (2016).
- [36] Oscar Moll, Favven Bastani, Sam Madden, Mike Stonebraker, Vijay Gadepally, and Tim Kraska. 2020. ExSample: Efficient Searches on Video Repositories through Adaptive Sampling. *CoRR* abs/2005.09141 (2020).
- [37] Omar Aziz Niamut, Emmanuel Thomas, Lucia D’Acunto, Cyril Concolato, Franck Denoual, and Seong Yong Lim. 2016. MPEG DASH SRD: spatial relationship description. In *MMSys*. ACM, 5:1–5:8.
- [38] nvenc [n.d.]. Nvidia Video codec. <https://developer.nvidia.com/nvidia-codec-sdk>.
- [39] OpenCV. 2018. Open Source Computer Vision Library. <https://opencv.org>.
- [40] Alex Poms, Will Crichton, Pat Hanrahan, and Kayvon Fatahalian. 2018. Scanner: efficient video analysis at scale. *ACM Trans. Graph.* 37, 4 (2018), 138:1–138:13.
- [41] Xukan Ran, Haoliang Chen, Xiaodan Zhu, Zhenming Liu, and Jiayi Chen. 2018. DeepDecision: A Mobile Deep Learning Framework for Edge Video Analytics. In *INFOCOM*. IEEE, 1421–1429.
- [42] Joseph Redmon and Ali Farhadi. 2018. YOLOv3: An Incremental Improvement. *CoRR* abs/1804.02767 (2018).
- [43] Andy Schuler and Matthew Donato. 2018. Engineers Making Movies (AKA Open Source Test Content). <https://netflixtechblog.com/engineers-making-movies-aka-open-source-test-content-f21363ea3781>. Accessed: 2020-06-01.
- [44] Gary J. Sullivan, Jens-Rainer Ohm, Woojin Han, and Thomas Wiegand. 2012. Overview of the High Efficiency Video Coding (HEVC) Standard. *TCSVT* 22, 12 (2012), 1649–1668.
- [45] VideoClarity. 2020. Understanding MOS, JND, and PSNR. <https://videoclarity.com/PDF/WPUnderstandingJNDMOSPSNR.pdf>. Accessed: 2020-06-01.
- [46] Mario Vranjes, Snjezana Rimac-Drlje, and Kresimir Grgic. 2008. Locally averaged PSNR as a simple objective Video Quality Metric. In *ELMAR*, Vol. 1. IEEE, 17–20.
- [47] Junjue Wang, Ziqiang Feng, Zhuo Chen, Shilpa Anna George, Mihir Bala, Padmanabhan Pillai, Shao-Wen Yang, and Mahadev Satyanarayanan. 2018. Bandwidth-Efficient Live Video Analytics for Drones Via Edge Computing. In *SEC*. IEEE, 159–173.
- [48] Xiaoli Wang, Aakanksha Chowdhery, and Mung Chiang. 2016. SkyEyes: adaptive video streaming from UAVs. In *HotWireless@MobiCom*. ACM, 2–6.
- [49] Susan Wojcicki. 2018. The Potential Unintended Consequences of Article 13. <https://youtube-creators.googleblog.com/2018/11/i-support-goals-of-article-13-i-also.html>.
- [50] Chao-Yuan Wu, Manzil Zaheer, Hexiang Hu, R. Manmatha, Alexander J. Smola, and Philipp Krähenbühl. 2018. Compressed Video Action Recognition. In *CVPR*. IEEE Computer Society, 6026–6035.
- [51] Ioannis Xarchakos and Nick Koudas. 2019. SVQ: Streaming Video Queries. In *SIGMOD*. ACM, 2013–2016.
- [52] Tiantu Xu, Luis Materon Botelho, and Felix Xiaozhu Lin. 2019. VStore: A Data Store for Analytics on Large Videos. In *EuroSys*. ACM, 16:1–16:17.
- [53] Haoyu Zhang, Ganesh Ananthanarayanan, Peter Bodik, Matthai Philipose, Paramvir Bahl, and Michael J. Freedman. 2017. Live Video Analytics at Scale

with Approximation and Delay-Tolerance. In *NSDI*. 377–392.

[54] Yuhao Zhang and Arun Kumar. 2019. Panorama: A Data System for Unbounded Vocabulary Querying over Video. *PVLDB* 13, 4 (2019), 477–491.